Frequency domain identification of autoregressive models in the presence of additive noise

Umberto Soverini[a], Torsten Söderström[b]

[a]*Department of Electrical, Electronic and Information Engineering, University of Bologna, Italy*
(e-mail: umberto.soverini@unibo.it)
[b]*Department of Information Technology, Uppsala University, Sweden*
(e-mail: ts@it.uu.se)

Abstract

This paper describes a new approach for identifying autoregressive models from a finite number of measurements, in presence of additive and uncorrelated white noise. As a major novelty, the proposed approach deals with frequency domain data. In particular, two different frequency domain algorithms are proposed. The first algorithm is based on some theoretical results concerning the so–called dynamic Frisch Scheme. The second algorithm maps the AR identification problem into a quadratic eigenvalue problem. Both methods resemble in many aspects some other identification algorithms, originally developed in the time domain. The features of the proposed methods are compared to each other and with those of other time domain algorithms by means of Monte Carlo simulations.

Keywords: System identification; Autoregressive models; Frisch Scheme; Discrete Fourier Transform.

1. Introduction

Autoregressive (AR) models are commonly used in the field of spectral analysis and find applications in a wide range of engineering problems, like, for example, speech analysis, radar and sonar systems, vibration monitoring, astronomy, geophysics and seismology.

In spectral analysis literature [1, 2, 3] two different methodologies are usually described. The first methodology contains the classical nonparametric approaches, involving periodogram and correlogram methods. The second methodology contains the parametric approaches, also called model–based. These methods postulate a model for the data, that constitutes a means for parameterizing the spectrum. The spectral estimation problem is thus reduced to the estimation of the parameters of the model.

Both methodologies offer advantages and disadvantages in order to obtain an accurate spectrum estimation with high resolution. They can be distinguished by the fact that nonparametric methods treat with frequency domain data, while parametric methods are commonly developed in the time domain, even if the identification of stochastic ARMA models can be approached from a frequency perspective as well [4, 5, 6, 7].

Within the class of parametric methods, AR models are widely used since they constitute the simplest description of a stochastic process and offer the possibility for simple and fast parameter identification procedures, based on least squares estimation schemes.

In many practical situations, however, simple AR models are not adequate since the signals are corrupted by noise. In these cases, classical AR identification methods give misleading results; in fact it can be proved that the estimated AR poles are biased toward the center of the unit circle, leading thus to a smoothed spectrum [8].

Several approaches have been developed to recover the AR parameters from noisy measurements. Since noisy AR processes admit an equivalent ARMA representation [9], some usual approaches for solving this problem consist in standard ARMA parameter estimators, like prediction errors methods [10].

Another classical approach for the identification of AR plus noise models consists in solving the so–called high–order Yule–Walker (HOYW) equations [11]. This method requires the knowledge of the autocorrelation function for high lags and is characterized by a poor estimate of the parameters. To compensate the estimation errors, an overdetermined set of HOYW equations is often considered [12]. In [13, 14, 15] it has been shown that better results can be obtained by using both low and high order YW equations. Starting from this set up, in [16] a new method has been proposed, related to signal/noise subspace techniques. This approach uses a modified set of low and high order YW equations and maps the original problem into a quadratic eigenvalue problem. The estimates of the AR parameters and of the noise variance are thus obtained by solving the associated generalized eigenvalue problem.

Other approaches for the identification of AR plus noise models are based on the so-called bias–compensation least–squares (BCLS) technique [17, 18, 19]. These methods make use of iterative least–squares procedures where, at each step, the current estimate of the noise variance is used for improving the estimate of the AR parameters and *vice versa*. A unified explanation of various BCLS schemes is reported in [20].

A different, not iterative, approach has been proposed in

[21, 22, 23]. In these papers the AR plus noise identification problem is solved by using the theoretical results concerning the so–called dynamic Frisch Scheme [24, 25] which was originally developed for the identification of errors–in–variables systems.

In this work the identification of AR systems corrupted by additive white noise is addressed by using a frequency domain approach. In particular, two different frequency domain algorithms are proposed and their features are compared to each other and with those of other time domain methods.

In presence of non periodic signals of finite length, leakage problems have been always considered to be the major drawback for frequency domain methods. In fact, leakage errors are present even in absence of disturbing noise. In this respect, an important result has been given in [26], where it has been proved that for a linear, discrete–time system, described by a rational transfer function of finite dimensions, the discrete Fourier transforms (DFTs) of the input–output signals are exactly linked by an extended model that includes also a polynomial term of finite order, that takes into account the leakage and transient effects.

From a theoretic point of view, this result has been formalized in [27], where the full equivalence between time and frequency domain identification methods was established, also for finite data records. However, from the practical point of view, the decision to implement a time or a frequency domain algorithm can strongly depend on the user choices and on the specific applications.

Frequency domain techniques for system identification are described in [7]. In most experimental situations the observations are collected as samples of time signals, so that a Fourier transformation is required before implementing a frequency domain algorithm. However, there exist occasions in which the data are more easily available as frequency samples. For example, in some experimental situations it may occur that the data are collected by a frequency analyzer which directly provides the Fourier transforms of the time signals. This situation is particularly common in vibrational analysis of mechanical systems [6].

Frequency domain approaches are characterized by some specific features that are not present in the time domain methods [28]. In particular, in the frequency domain the filtering operations are quite simple to implement, in fact they can be reduced to the selection of appropriate (weighted) frequencies in a limited band of the signal spectrum. As a consequence, frequency domain approaches allow to solve in a more direct and simple way all the problems where a trade–off between frequency resolution and noise level is present. This feature can be of great advantage in the identification of noisy AR processes with narrowband spectrum, as will be illustrated by a numerical example.

The organization of the paper is as follows. Section 2 defines the AR plus noise identification problem in the frequency domain, while Section 3 introduces a novel frequency domain description of the AR processes. In Section 4 the identification problem is reformulated as a Frisch Scheme problem and the search for the solution is analyzed within this context. Sections 5 describes a possible identification criterion, that can be directly formulated in the frequency domain. In particular, this criterion takes advantage of a set of equations similar to the HOYW equations. For this reason the method can be considered the frequency counterpart of the time domain approach proposed in [22, 23]. In Section 6, it is shown how the AR identification problem can be reformulated as a quadratic eigenvalue problem involving only the output noise variance. The obtained quadratic eigenvalue problem is thus solved by mapping it into a generalized eigenvalue problem. The method can be considered to be the frequency counterpart of the time domain approach proposed in [16]. In Section 7 the effectiveness of the proposed methods is verified by means of Monte Carlo simulations. It is shown that this new frequency domain methodology is characterized by high frequency resolution properties and is particularly suited for the identification of narrowband AR systems with close and sharp spectral peaks. Finally some concluding remarks are reported in Section 8.

2. Statement of the problem

Consider the following noisy AR model, of order n, described by the equations

$$x(t) = -\alpha_1\, x(t-1) - \cdots - \alpha_n\, x(t-n) + e(t) \tag{1}$$

$$y(t) = x(t) + w(t) \tag{2}$$

where $x(t)$ is the output of the noise–free AR model, driven by the white noise process $e(t)$. The available observation $y(t)$ is affected by the noise process $w(t)$.

The following assumptions are applied.

A1. $e(t)$ is a zero–mean ergodic white process, with *unknown* variance σ_e^*.

A2. The order n of the AR model is assumed as *a priori* known.

A3. The additive noise $w(t)$ is a zero–mean ergodic white process, uncorrelated with $e(t)$, with *unknown* variance σ_w^*.

Let $\{y(t)\}_{t=0}^{N-1}$ be a set of noisy observations at N equidistant time instants. The corresponding Discrete Fourier Transform (DFT) is defined as

$$Y(\omega_k) = \frac{1}{\sqrt{N}} \sum_{t=0}^{N-1} y(t)\, \mathrm{e}^{-j\omega_k t}\,, \tag{3}$$

where $\omega_k = 2\pi k/N$ and $k = 0, \ldots, N-1$.

In the frequency domain, the problem under investigation can be stated as follows.

Problem 1. Let $Y(\omega_k)$ be a set of noisy measurements generated by an AR plus noise system of type (1)–(2), under assumptions A1–A3, where $\omega_k = 2\pi k/N$ and $k = 0, \ldots, N-1$. Estimate the AR parameters α_i $(i = 1, \ldots, n)$ and the noise variances σ_e^*, σ_w^*.

3. A frequency domain setup

In this Section a new frequency domain description for the noisy AR model (1)–(2) is introduced. This setup has been originally developed in [30, 31, 29] with reference to the identification of errors–in–variables systems.

Equation (1) can be rewritten as

$$A(z^{-1})x(t) = e(t) \tag{4}$$

where $A(z^{-1})$ is a polynomial in the backward shift operator z^{-1}

$$A(z^{-1}) = 1 + \alpha_1 z^{-1} + \cdots + \alpha_n z^{-n}. \tag{5}$$

It can be noted that equation (4) defines a dynamic system, where

$$G(\mathrm{e}^{-j\omega_k}) = \frac{1}{A(\mathrm{e}^{-j\omega_k})} \tag{6}$$

is the transfer function between the output $x(t)$ and the input $e(t)$.

With reference to the signals $e(t)$ and $x(t)$, define the corresponding DFTs

$$E(\omega_k) = \frac{1}{\sqrt{N}} \sum_{t=0}^{N-1} e(t)\, \mathrm{e}^{-j\omega_k t} \tag{7}$$

$$X(\omega_k) = \frac{1}{\sqrt{N}} \sum_{t=0}^{N-1} x(t)\, \mathrm{e}^{-j\omega_k t}\,, \tag{8}$$

where $\omega_k = 2\pi k/N$ and $k = 0, \ldots, N-1$.

It is a well–known fact [26] that for finite N, even in absence of noise, the ratio of the DFTs $X(\omega_k)$ and $E(\omega_k)$ is not equal to the true transfer function

$$G(\mathrm{e}^{-j\omega_k}) \neq \frac{X(\omega_k)}{E(\omega_k)}\,. \tag{9}$$

In fact, it can be proved that the DFTs $X(\omega_k)$ and $E(\omega_k)$ exactly satisfy an extended model that includes also a transient term, i.e.

$$A(\mathrm{e}^{-j\omega_k})\, X(\omega_k) = E(\omega_k) + T(\mathrm{e}^{-j\omega_k})\,, \tag{10}$$

where $T(z^{-1})$ is a polynomial of order $n-1$

$$T(z^{-1}) = \tau_0 + \tau_1 z^{-1} + \cdots + \tau_{n-1} z^{-n+1} \tag{11}$$

that takes into account the effects of the initial and final conditions of the experiment.

By considering the whole number of frequencies, eq. (10) can be rewritten in a matrix form. For this purpose, introduce the parameter vectors

$$\theta_\alpha = [1\, \alpha_1 \ldots \alpha_n]^T \tag{12}$$

$$\theta_\tau = [\tau_0 \ldots \tau_{n-1}]^T\,. \tag{13}$$

and define the following vector Θ, with dimension $p = 2n+1$, containing the whole number of parameters

$$\Theta = [\ \theta_\alpha^T\ -\theta_\tau^T\ ]^T\,. \tag{14}$$

In absence of noise, the AR parameters can be recovered by means of the following procedure. Define the row vectors

$$Z_{n+1}(\omega_k) = [1\ \mathrm{e}^{-j\omega_k}\ \ldots\ \mathrm{e}^{-j(n-1)\omega_k}\ \mathrm{e}^{-jn\omega_k}\ ] \tag{15}$$

$$Z_n(\omega_k) = [1\ \mathrm{e}^{-j\omega_k}\ \ldots\ \mathrm{e}^{-j(n-1)\omega_k}\ ]\,, \tag{16}$$

whose entries are constructed with multiple frequencies of ω_k, and construct the following matrices

$$\Pi = \begin{bmatrix} Z_{n+1}(\omega_0) \\ \vdots \\ Z_{n+1}(\omega_{N-1}) \end{bmatrix} \qquad \Psi = \begin{bmatrix} Z_n(\omega_0) \\ \vdots \\ Z_n(\omega_{N-1}) \end{bmatrix}\,. \tag{17}$$

of dimension $N \times (n+1)$ and $N \times n$, respectively.

With the DFT samples (8) construct the following $N \times N$ diagonal matrix

$$V_X^{diag} = \mathrm{diag}\,[X(\omega_0),\, X(\omega_1), \ldots, X(\omega_{N-1})] \tag{18}$$

and compute the $N \times (n+1)$ matrix

$$\Pi_X = V_X^{diag}\, \Pi\,. \tag{19}$$

Then, construct the $N \times p$ matrix

$$\Phi_X = [\ \Pi_X \,|\, \Psi\ ]\,. \tag{20}$$

Thus, eq. (10) can be rewritten as

$$\Phi_X\, \Theta = V_E\,. \tag{21}$$

Define now the $p \times p$ matrix

$$\Sigma_X = \frac{1}{N}(\Phi_X^H\, \Phi_X)\,, \tag{22}$$

where $(\cdot)^H$ denotes the transpose and conjugate operation.

Because of assumption A1, when $N \to \infty$, from (21) it follows that

$$\bar{\Sigma}_X\, \Theta = 0\,, \tag{23}$$

where $\bar{\Sigma}_X$ is defined as

$$\bar{\Sigma}_X = \Sigma_X - \mathrm{diag}\,[\ \sigma_e^*\ \underbrace{0\ \ldots\ 0}_{2n}\ ]\,. \tag{24}$$

Remark 1. Since $x(t)$ is generated by the AR model (4), relation (10) cannot be satisfied by a polynomial $A(z^{-1})$ with order lower than n. Therefore, matrix $\bar{\Sigma}_X$ in (24) is positive semidefinite, with only one null eigenvalue, i.e.

$$\bar{\Sigma}_X \geq 0 \qquad \dim \ker \bar{\Sigma}_X = 1\,. \tag{25}$$

In presence of noise, the previous procedure can be modified as follows. With the DFT samples (3) construct the $N \times N$ diagonal matrix

$$V_Y^{diag} = \mathrm{diag}\,[Y(\omega_0),\, Y(\omega_1), \ldots, Y(\omega_{N-1})] \tag{26}$$

and compute the matrix

$$\Pi_Y = V_Y^{diag}\, \Pi\,. \tag{27}$$

Then, construct the $N \times p$ matrix

$$\Phi_Y = [\, \Pi_Y \,|\, \Psi \,] \,. \tag{28}$$

Because of Assumptions A3, when $N \to \infty$, we obtain the following $p \times p$ positive definite matrix

$$\Sigma_Y = \frac{1}{N}(\Phi_Y^H \, \Phi_Y) = \Sigma_X + \begin{bmatrix} \sigma_w^* \, I_{n+1} & 0 \\ 0 & 0_n \end{bmatrix} , \tag{29}$$

where 0_n is the null square matrix of dimension n.

By combining (24) and (29), it follows that

$$\Sigma_Y = \bar{\Sigma}_X + \tilde{\Sigma}^* \,, \tag{30}$$

where

$$\tilde{\Sigma}^* = \begin{bmatrix} \sigma_s^* & 0 & 0 \\ 0 & \sigma_w^* \, I_n & 0 \\ 0 & 0 & 0_n \end{bmatrix} \tag{31}$$

and

$$\sigma_s^* = \sigma_w^* + \sigma_e^* \,. \tag{32}$$

From (23) and (30), the parameter vector Θ, defined in (14), can be obtained as the kernel of

$$(\Sigma_Y - \tilde{\Sigma}^*) \, \Theta = 0 \,, \tag{33}$$

after normalizing the first entry to 1.

Remark 2. It can be observed that for $k = 0, \ldots, \text{floor}\,(\frac{N-1}{2})$

$$\begin{aligned} Y(\omega_{N-1-k}) &= \frac{1}{\sqrt{N}} \sum_{t=0}^{N-1} y(t) \, \mathrm{e}^{-j \frac{N-1-k}{N} 2\pi t} \\ &= \frac{1}{\sqrt{N}} \sum_{t=0}^{N-1} y(t) \, \mathrm{e}^{-j \frac{-(1+k)}{N} 2\pi t} = Y^*(\omega_{1+k}) \,, \end{aligned} \tag{34}$$

where $Y^*(\cdot)$ is the conjugate of $Y(\cdot)$. Consequently, a redundant information has been used in the definition (29) of Σ_Y and only the first $N/2$ samples $Y(\omega_k)$, $k = 0, \ldots, \text{floor}\,(\frac{N-1}{2})$, could be considered. However, from simulation experiences the usage of the whole data set $Y(\omega_k)$, $k = 0, \ldots, N-1$, leads to better results, especially under the conditions described in Remark 3.

4. Analysis in the Frisch Scheme context

Starting from knowledge of the noisy matrix Σ_Y, the determination of the system parameter vector Θ and of the noise variances σ_e^*, σ_w^* can be seen as a Frisch Scheme problem [24, 25].

Consider the set of non–negative definite diagonal matrices of type

$$\tilde{\Sigma} = \text{diag}\,[\, \sigma_s, \, \sigma_w \, I_n, \, 0_n \,] \tag{35}$$

such that

$$\Sigma_Y - \tilde{\Sigma} \geq 0 \qquad \det\,(\Sigma_Y - \tilde{\Sigma}) = 0 \,. \tag{36}$$

With the same reasoning of [24], the following statements can be proved.

Theorem 1. The set of all matrices $\tilde{\Sigma}$ satisfying conditions (36) defines the points $P = (\sigma_s, \sigma_w)$ of a convex curve $\mathcal{S}(\Sigma_Y)$ belonging to the first quadrant of the noise space $\mathcal{R}^2$ whose concavity faces the origin. At every point $P = (\sigma_s, \sigma_w)$ can be associated the noise matrix $\tilde{\Sigma}(P)$ and the coefficient vector $\Theta(P)$ satisfying the relation

$$\left(\Sigma_Y - \tilde{\Sigma}(P)\right) \Theta(P) = 0 \,. \, \Diamond \tag{37}$$

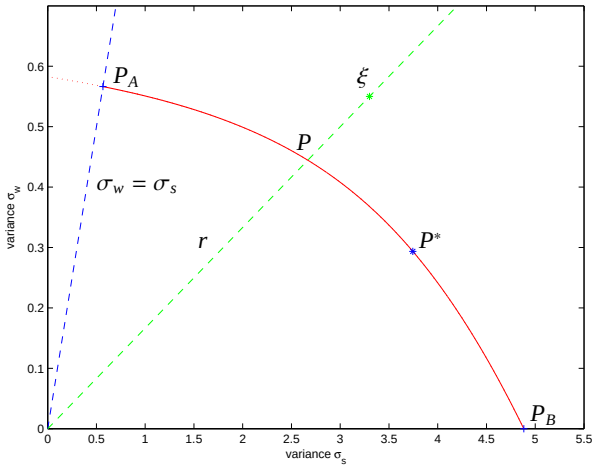

Figure 1: Typical shape of $\mathcal{S}(\Sigma_Y)$.

Proof. See [24].

Theorem 2. Because of the relations (31)–(33), the point $P^* = (\sigma_s^*, \sigma_w^*)$, associated with the true variances of $e(t)$ and $w(t)$, belongs to $\mathcal{S}(\Sigma_Y)$ and the corresponding coefficient vector $\Theta(P^*)$ is characterized (after a normalization of its first entry to 1) by the true system parameter vector, i.e. $\Theta(P^*) = \Theta$. $\Diamond$

Proof. See [24].

In Figure 1 an example of $\mathcal{S}(\Sigma_Y)$ is reported. Note that the points (σ_s, σ_w) of the curve with $\sigma_s \leq \sigma_w$ (dotted line) are non admissible because they do not satisfy the condition $\sigma_e = \sigma_s - \sigma_w > 0$. The set of admissible solutions (continuous line) is thus delimited by the straight lines $\sigma_w = \sigma_s$ and $\sigma_w = 0$.

Theorem 3. Partition the matrix Σ_Y as follows

$$\Sigma_Y = \begin{bmatrix} \sigma_{11} & \Sigma_{12} \\ \Sigma_{21} & \Sigma_{22} \end{bmatrix} \tag{38}$$

where Σ_{22} is the square matrix of dimension $2n$. The intersection of $\mathcal{S}(\Sigma_Y)$ with the σ_s axis is the point $P_B = (\sigma_s^{max}, 0)$ given by the least squares solution

$$\sigma_s^{max} = \frac{\det\,(\Sigma_Y)}{\det\,(\Sigma_{22})} \,. \tag{39}$$

Partition the matrix Σ_Y instead as follows

$$\Sigma_Y = \begin{bmatrix} \Sigma_{11} & \Sigma_{12} \\ \Sigma_{21} & \Sigma_{22} \end{bmatrix} \tag{40}$$

where Σ_{22} is the square matrix of dimension n. The intersection of $\mathcal{S}(\Sigma_Y)$ with the straight line $\sigma_w = \sigma_s$ is the point $P_A = (\sigma_w^{max}, \sigma_w^{max})$, given by the solution

$$\sigma_w^{max} = \min \text{ eig}\left(\Sigma_{11} - \Sigma_{12} \, \Sigma_{22}^{-1} \, \Sigma_{21}\right) . \tag{41}$$

Since the point P_A corresponds to $\sigma_e = 0$, it is not a solution of Problem 1. $\Diamond$

Proof. The proof is provided in Appendix A.

The next theorem describes a parametrization of the curve $\mathcal{S}(\Sigma_Y)$ that allows to associate a solution of (36) with every straight line departing from the origin and lying in the first quadrant [25]. This parametrization plays an important role in the practical implementation of the identification algorithm.

Theorem 4. Let $\xi = (\xi_1, \xi_2)$ be a generic point of the first quadrant of $\mathcal{R}^2$ and r the straight line from the origin through ξ (see Fig. 1). Its intersection with $\mathcal{S}(\Sigma_Y)$ is the point $P = (\sigma_s, \sigma_w)$ given by

$$\sigma_s = \frac{\xi_1}{\lambda_M} \qquad \sigma_w = \frac{\xi_2}{\lambda_M} , \tag{42}$$

where

$$\lambda_M = \max \operatorname{eig}\left(\Sigma_Y^{-1}\tilde{\Sigma}_\xi\right) \tag{43}$$

$$\tilde{\Sigma}_\xi = \begin{bmatrix} \xi_1 & 0 & 0 \\ 0 & \xi_2 I_n & 0 \\ 0 & 0 & 0_n \end{bmatrix} . \Diamond \tag{44}$$

Proof. The proof is provided in Appendix B.

Remark 3. The described procedure allows to construct the curve $\mathcal{S}(\Sigma_Y)$ in the noise space (σ_s, σ_w) also when only a subset of the whole frequency range is used, on condition that the number of the selected frequencies is large enough. This subset must be chosen by the user on the basis of *a priori* knowledge of the frequency properties of the transfer function $G(e^{-j\omega_k})$ defined in (6). In practice, taking into account the observations of Remark 2, two distinct sets of frequencies are jointly considered, the set $W_1 = [\omega_i, \omega_f]$, with $i \geq 0$ and $f \leq \text{floor}\,(\frac{N-1}{2})$ and the set $W_2 = [\omega_{N-1-f}, \omega_{N-1-i}]$, for a total number of the $2L$ frequencies, with $L = f - i + 1$. By considering a new matrix Φ_Y with $2L$ rows, expressions (29)–(31) must be modified as follows

$$\Sigma_Y = \frac{1}{2L}(\Phi_Y^H \Phi_Y) = \bar{\Sigma}_X + \tilde{\Sigma}^* , \tag{45}$$

where

$$\tilde{\Sigma}^* = \frac{N}{2L}\begin{bmatrix} \sigma_s^* & 0 & 0 \\ 0 & \sigma_w^* I_n & 0 \\ 0 & 0 & 0_n \end{bmatrix} . \tag{46}$$

5. A criterion based on HOYW–type equations

As asserted in Theorem 2, the determination of the point P^* on $\mathcal{S}(\Sigma_Y)$ leads to the solution of Problem 1. For this purpose a search criterion must be introduced. Unfortunately, the theoretic properties of $\mathcal{S}(\Sigma_Y)$ described so far do not allow to distinguish the point P^* from the other points of the curve.

In this section we will describe a possible search criterion. This criterion is analogue to that reported in [22] with reference to time domain identification of AR plus noise models.

Select the integer $q \geq 2n$. Analogously to (15), consider the row vector

$$Z_{q+n+1}(\omega_k) = [1\ e^{-j\omega_k}\ \ldots e^{-j(n+q)\omega_k}] \tag{47}$$

and extract from it the q–dimensional row vector

$$Z_q^h(\omega_k) = [e^{-j(n+1)\omega_k}\ \ldots e^{-j(n+q)\omega_k}] . \tag{48}$$

Then, construct the following $N \times q$ matrix

$$\Pi^h = \begin{bmatrix} Z_q^h(\omega_0) \\ \vdots \\ Z_q^h(\omega_{N-1}) \end{bmatrix} . \tag{49}$$

and compute the $N \times q$ matrix

$$\Phi_X^h = V_X^{diag}\,\Pi^h . \tag{50}$$

Define now the $q \times p$ matrix

$$\Sigma_X^h = \frac{1}{N}((\Phi_X^h)^H \Phi_X) , \tag{51}$$

Because of assumption A1, when $N \to \infty$, it follows that

$$\Sigma_X^h\,\Theta = 0 . \tag{52}$$

In an analogous way, we can compute the $N \times q$ matrix

$$\Phi_Y^h = V_Y^{diag}\,\Pi^h \tag{53}$$

and define the $q \times p$ matrix

$$\Sigma_Y^h = \frac{1}{N}((\Phi_Y^h)^H \Phi_Y) . \tag{54}$$

Because of Assumptions A3, when $N \to \infty$, it holds

$$\Sigma_Y^h = \Sigma_X^h . \tag{55}$$

It is thus possible to write

$$\Sigma_Y^h\,\Theta = 0 . \tag{56}$$

Equation (56) constitutes a set of q equations, analogue to the time domain high order Yule–Walker equations, that does not involve the output noise variance σ_w^*.

Thanks to this property the search for P^* along $\mathcal{S}(\Sigma_Y)$ can be performed by introducing the following cost function

$$J(P) = \|\Sigma_Y^h\,\Theta(P)\|_2^2 = \Theta^T(P)(\Sigma_Y^h)^H\,\Sigma_Y^h\,\Theta(P) . \tag{57}$$

Remark 4. When $q \geq 2n$ the cost function $J(P)$ in (57) exhibits the following properties

i) $J(P) \geq 0$

ii) $J(P) = 0 \Leftrightarrow P = P^*$.

In fact, if $q \geq 2n$ the conditions stated in [32] hold and the equation (56) admits a unique solution, corresponding to the true system parameter Θ.

Remark 5. Equations (56) could be directly used to obtain an estimate of the parameter vector Θ if $q \geq 2n$. This approach is analogue to an instrumental variable (IV) method in the time domain, where delayed outputs are used as instruments. These equations can be solved by using a total least squares approach

[33]. The main advantage of the method is the computational efficiency. On the other hand, the obtained estimation accuracy is often poor [34].

On the basis of the previous considerations, it is thus possible to develop the following algorithm.

Algorithm 1.

1. Compute, on the basis of the available data $Y(\omega_k)$ with $\omega_k = 2\pi k/N$ ($k = 0, \ldots, N-1$), the matrix Π_Y as in (27) and construct the matrix Φ_Y as in (28).
2. Compute, as in (29), the sample estimate of matrix

$$\Sigma_Y = \frac{1}{N}\left(\Phi_Y^H \Phi_Y\right) . \tag{58}$$

3. Select $q \geq 2n$ and construct the matrix Π^h as in (49), then compute Φ_Y^h as in (53).
4. Compute, as in (54), the sample estimate of matrix

$$\Sigma_Y^h = \frac{1}{N}\left((\Phi_Y^h)^H \Phi_Y\right) . \tag{59}$$

5. Start from a generic point ξ (a generic direction) in the first quadrant of $\mathcal{R}^2$ and compute, by means of (42)–(44) the corresponding point $P = (\sigma_s, \sigma_w)$ on $\mathcal{S}(\Sigma_Y)$.
6. Compute the estimates of $\bar{\Sigma}_X(P)$ and $\Theta(P)$ by means of the relations

$$\bar{\Sigma}_X(P) = \Sigma_Y - \mathrm{diag}\left[\, \sigma_s,\, \sigma_w I_n,\, 0_n \,\right], \tag{60}$$

$$\bar{\Sigma}_X(P)\,\Theta(P) = 0 . \tag{61}$$

7. Compute the value of the cost function $J(P)$ (57).
8. Search on the curve $\mathcal{S}(\Sigma_Y)$ for the point P° associated with the minimum of $J(P)$.

6. A subspace approach

The approach proposed in this section is analogue to that described in [16] and exploits the set of equations (56) together with the equations (33). It will be shown that the AR plus noise identification problem can be mapped into a quadratic eigenvalue problem that, in turn, can be solved as a generalized eigenvalue problem. The system parameters are thus estimated in one shot, without any search procedure.

Let us partition matrix Σ_Y, defined in (29), as follows

$$\Sigma_Y = \begin{bmatrix} \sigma_{11} & \Sigma_{12} & \Sigma_{13} \\ \Sigma_{21} & \Sigma_{22} & \Sigma_{23} \\ \Sigma_{31} & \Sigma_{32} & \Sigma_{33} \end{bmatrix} , \tag{62}$$

where σ_{11} is a scalar and Σ_{22}, Σ_{33} are square matrices of dimension n.

By analyzing the structure of matrix (31), it can be observed that, when $N \to \infty$, the last $2n$ equations in (33) can be written as

$$\begin{bmatrix} \Sigma_{21} & \Sigma_{22} - \sigma_w^* I_n & \Sigma_{23} \\ \Sigma_{31} & \Sigma_{32} & \Sigma_{33} \end{bmatrix} \Theta = 0 . \tag{63}$$

Equation (63) contains $2n+1$ unknowns, i.e. σ_w^* and the entries of Θ. By choosing $q \geq 1$, the equations (56) can be combined with the equations (63) in order obtain the following nonlinear system of $2n + q$ equations

$$\begin{bmatrix} \Sigma_{21} & \Sigma_{22} - \sigma_w^* I_n & \Sigma_{23} \\ \Sigma_{31} & \Sigma_{32} & \Sigma_{33} \\ & \Sigma_Y^h & \end{bmatrix} \Theta = 0 . \tag{64}$$

This set of equations can be rewritten as

$$(S - \sigma_w^* J)\,\Theta = 0, \tag{65}$$

where

$$S = \begin{bmatrix} \Sigma_{21} & \Sigma_{22} & \Sigma_{23} \\ \Sigma_{31} & \Sigma_{32} & \Sigma_{33} \\ & \Sigma_Y^h & \end{bmatrix} \tag{66}$$

$$J = \begin{bmatrix} 0_{n\times 1} & I_n & 0_n \\ 0_{n\times 1} & 0_n & 0_n \\ & 0_{q\times(2n+1)} & \end{bmatrix} . \tag{67}$$

Multiplying both sides of (65) by $(S - \sigma_w^* J)^T$ leads to the equation

$$\left(A_2\,\sigma_w^{2*} + A_1\,\sigma_w^* + A_0\right)\Theta = 0, \tag{68}$$

where

$$A_0 = S^T S \tag{69}$$

$$A_1 = -\left(S^T J + J^T S\right) \tag{70}$$

$$A_2 = J^T J. \tag{71}$$

The coefficients of Θ can thus be estimated by solving the following quadratic eigenvalue problem (QEP)

$$\left(A_2\,\lambda^2 + A_1\,\lambda + A_0\right) v = 0. \tag{72}$$

The set of $4n + 2$ eigenvalues solving (72) are real or appear in complex conjugate pairs and can also be infinite [35]. If the system is identifiable and the number of data $N \to \infty$, the only real eigenvalue (with multiplicity two) that solves (72) is $\lambda = \sigma_w^*$. It is thus possible to conclude that the solution of the identification problem is the eigenvector associated with the only real eigenvalue that solves (72).

The QEP (72) can be solved in several ways [35]. The easiest way to solve it consists in rewriting equation (72) as

$$A_2\,v'\,\lambda + A_1\,v\,\lambda + A_0\,v = 0, \tag{73}$$

where $v' = \lambda\, v$. Thus, the following $(4n+2)$–dimensional linear generalized eigenvalue problem (GEP) can be derived [35]

$$(P - \lambda\, Q)\;\eta = 0, \tag{74}$$

where

$$P = \begin{bmatrix} A_0 & 0 \\ 0 & I_{2n+1} \end{bmatrix} \tag{75}$$

$$Q = \begin{bmatrix} -A_1 & -A_2 \\ I_{2n+1} & 0 \end{bmatrix} \tag{76}$$

$$\eta = \left[\, v^T \;\; v'^T \,\right]^T. \tag{77}$$

The only real eigenvalue solving (74) is σ_w^* and the first $2n+1$ entries of the corresponding eigenvector η^* are, after a normalization of the first entry to 1, the entries of Θ, i.e.

$$\eta_0 = \frac{\eta^*}{\eta^*(1)} = [\ \Theta^T \ \ \sigma_w^* \Theta^T\ ]^T. \tag{78}$$

Remark 6. Since only a finite number N of data is available, all the eigenvalues solving (74) will exhibit, in general, a small imaginary part. A criterion leading to good results consists in choosing the eigenvalue having the smallest modulus [16].

The whole identification procedure can be summarized as follows.

Algorithm 2.

1. Compute, on the basis of the available data $Y(\omega_k)$ with $\omega_k = 2\pi k/N$ ($k = 0, \ldots, N-1$), the matrix Π_Y as in (27) and construct the matrix Φ_Y as in (28).
2. Compute, as in (29), the sample estimate of matrix

$$\Sigma_Y = \frac{1}{N}\left(\Phi_Y^H \Phi_Y\right). \tag{79}$$

3. Select $q \geq 1$ and construct the matrix Π^h as in (49), then compute Φ_Y^h as in (53).
4. Compute, as in (54), the sample estimate of matrix

$$\Sigma_Y^h = \frac{1}{N}\left((\Phi_Y^h)^H \Phi_Y\right). \tag{80}$$

5. Construct the matrices S and J as in (66)–(67) and compute the matrices A_0, A_1, A_2 (69)–(71).
6. Construct the matrices P and Q as in (75)–(76).
7. Solve the generalized eigenvalue problem

$$(P - \lambda\, Q)\ \eta = 0, \tag{81}$$

   and choose as estimate of σ_w^* the modulus of the generalized eigenvalue having minimum modulus. Let η^* be the corresponding eigenvector.
8. Divide η^* by the first entry $\eta^*(1)$ in order to obtain an estimate of Θ, as in (78)

$$\eta_0 = [\ \Theta^T\ \#]^T\ , \tag{82}$$

   where # denotes the last $2n+1$ entries of $\eta^*/\eta^*(1)$, which are not of interest.
9. Starting from (62), consider the first equation of (33)

$$\left[\ \sigma_{11} - \sigma_w^* - \sigma_e^* \quad \Sigma_{12} \quad \Sigma_{13}\ \right]\Theta = 0 \tag{83}$$

   and solve it with respect to the unknown σ_e^*.

7. Numerical examples

In this section, the effectiveness of the proposed identification algorithms is tested by means of numerical simulations.

Example 1. The proposed algorithms have been tested on sequences generated by the following AR model of order $n = 4$, already considered in [22]

$$\begin{aligned} x(t) =& 2.4\, x(t-1) - 3.03\, x(t-2) + 1.986\, x(t-3) \\ &- 0.6586\, x(t-4) + e(t)\ , \end{aligned} \tag{84}$$

where $e(t)$ is a white noise with variance $\sigma_e^* = 1$.

A Monte Carlo simulation of 100 runs has been performed by using, in every run, $N = 1000$ samples of the noisy output $y(t)$. The variance of the observation noise is $\sigma_w^* = 4$, corresponding to a Signal to Noise Ratio (SNR) of about 10 dB, where the SNR is defined as

$$\mathrm{SNR} = 20\ \log_{10}\ \sqrt{\frac{E[x^2(t)]}{E[w^2(t)]}} = 10\ \log_{10}\ \frac{r_x(0)}{\sigma_w^*}\ \mathrm{dB}. \tag{85}$$

Table 1 reports the empirical means of the system parameter estimates and of the noise variance estimates, together with the corresponding standard deviations, obtained with the Algorithm 1, denoted with Alg1-FD, and with the Algorithm 2, denoted with Alg2-FD. The results are also compared with those obtained by the corresponding time domain algorithms described in [22] and [16] respectively, and denoted with Alg1-TD and Alg2-TD.

The table shows the results obtained when q is equal to the minimum number of equations required for the algorithms' implementation. It can be observed that Alg1-FD and Alg1-TD yield comparable results. Moreover, it can be noted that Alg2-FD yields completely wrong estimates when q is fixed to the minimum admissible value (third line in the Table). However, it is sufficient to select $q = n$ for obtaining parameter estimates that are comparable with those obtained by Alg2-TD and by the other methods.

Example 2. As a second example, the features of the new identification methods have been illustrated by means of the following 4–th order model, already proposed in [23]

$$\begin{aligned} x(t) =& 2.1690\, x(t-1) - 2.8227\, x(t-2) + 2.0408\, x(t-3) \\ &- 0.8853\, x(t-4) + e(t)\ , \end{aligned} \tag{86}$$

where $e(t)$ is a white noise with variance $\sigma_e^* = 1$. Model (86) describes a narrowband AR process.

The performances of the proposed methods have been evaluated by varying the number of the available data, with $N = 250$, $N = 500$, $N = 750$ and $N = 1000$. For every value of N, a Monte Carlo simulation of $N_r = 100$ independent runs has been performed. In all the simulations, the variance of the observation noise σ_w^* has been fixed in order to obtain SNR=10 dB, see (85).

With reference to the parameters vector θ_α, defined in (12), the performances of the estimation algorithms have been compared by means of the normalized root mean square error

$$\mathrm{NRMSE} = \frac{1}{\|\theta_\alpha\|}\ \sqrt{\frac{1}{N_r}\sum_{i=1}^{N_r} \|\hat{\theta}_\alpha^i - \theta_\alpha\|^2}, \tag{87}$$

Table 1: True and estimated values of parameters and variances for Alg1-FD, Alg2-FD and Alg1-TD, Alg2-TD. SNR ≈ 10 dB and N=1000.

	α_1	α_2	α_3	α_4	σ_e^*	σ_w^*	Time (ms)
true	−2.4	3.03	−1.986	0.6586	1	4	
Alg1 – FD ($q = 8$)	−2.3794 ± 0.1152	2.9969 ± 0.1693	−1.9569 ± 0.1278	0.6563 ± 0.0281	1.0921 ± 0.3272	4.0135 ± 0.1561	31.5
Alg1 – TD ($q = 4$)	−2.3864 ± 0.0325	3.0049 ± 0.1071	−1.9613 ± 0.1369	0.6553 ± 0.0960	0.9912 ± 0.0546	3.9646 ± 0.2184	8.0
Alg2 – FD ($q = 1$)	−0.9959 ± 0.0941	0.4582 ± 0.1318	0.3351 ± 0.1011	−0.1464 ± 0.0333	10.3536 ± 1.5160	1.5068 ± 0.6809	4.5
Alg2 – FD ($q = 4$)	−2.3913 ± 0.0367	3.0267 ± 0.0776	−1.9877 ± 0.0754	0.6714 ± 0.0366	1.0049 ± 0.4341	3.9769 ± 0.2297	5.5
Alg2 – TD ($q = 4$)	−2.3924 ± 0.0376	3.0234 ± 0.0732	−1.9824 ± 0.0688	0.6672 ± 0.0317	1.0256 ± 0.3870	3.9758 ± 0.2130	1.2

where $\hat{\theta}_\alpha^i$ denotes the estimate of θ_α obtained in the i–th trial of the Monte Carlo simulation.

Figure 2 reports the NRMSE versus the number of samples N. The figure reports also the values of the NMRSE obtained with Alg1-TD and Alg2-TD. It can be observed that all methods give comparable results.

For completeness, Table 2 reports the empirical means of the system parameter estimates and of the noise variance estimates, together with the corresponding standard deviations, obtained with Alg1-FD, Alg2-FD, Alg1-TD and Alg2-TD, when $N = 500$ and $\sigma_w^* = 3.6$, corresponding to a SNR of about 10 dB.

In Tables 1 and 2, the last column reports the mean value (in ms) of the time requested to carry out a single run of the Monte Carlo simulation. This value strongly depends on the specific features of the PC used for the simulations and, moreover, it may slightly change in different Monte Carlo sessions. However, it provides the correct order of magnitude of the computational efficiency of the algorithms and allows to make a comparison of their performances.

As shown in Tables 1 and 2, the estimation accuracy of the frequency domain algorithms Alg1-FD, Alg2-FD is comparable to that of the corresponding time domain algorithms Alg1-TD, Alg2-TD. However, as far as the computational efficiency is concerned, it must be observed that Alg2 is always much faster than Alg1, both in time and frequency domain. Moreover, the time domain algorithms are, approximatively, 4–5 times faster than the corresponding frequency domain implementations. Of course, in this respect, particular attention must be given to the coding. For example, it is worth noting that matrices Π_Y (27) and Φ_Y^h (53) must not be computed with the reported expressions, since highly time consuming.

Remark 7. It can be observed that the steps of each time domain algorithm are quite similar to those of the corresponding frequency domain version. Thus, it must be concluded that the major computational burden for the frequency domain approaches is mainly due to the following two facts: the preliminary DFT operations on the data, the computations developed in the complex domain. It cannot be excluded that the computational performances of the frequency domain approaches could be further improved by means of *ad hoc* implementations, suited for complex data elaborations.

This (modest) drawback is highly compensated by the fact that in the frequency domain the filtering operations can be implemented in a straightforward way, with great benefits for the identification, as it will be shown in the next example.

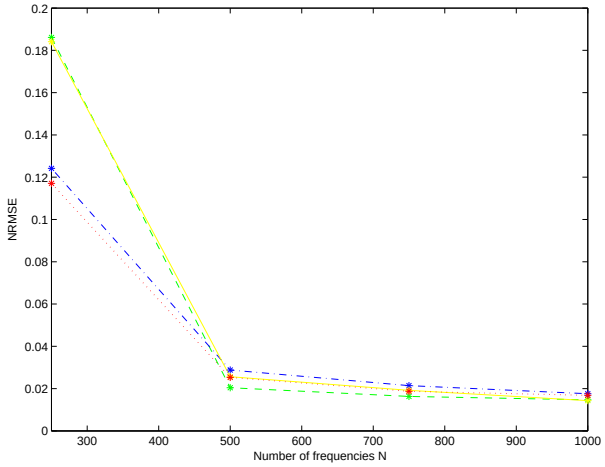

Figure 2: Alg1-FD: green, dashed; Alg2-FD: blue, dash–dotted, Alg1-TD: yellow, solid, Alg2-TD: red, dotted.

Example 3. In order to verify the selective properties described in Remark 3, the following AR model of order $n = 4$, also proposed in [13], has been considered

$$\begin{aligned} x(t) =& 2.7607\, x(t-1) - 3.8106\, x(t-2) + 2.6535\, x(t-3) \\ & - 0.9238\, x(t-4) + e(t)\,, \end{aligned} \tag{88}$$

where $e(t)$ is a white noise with variance $\sigma_e^* = 1$.

The model (88) exhibits two pairs of complex poles, with $p_{1,2} = 0.98\, \mathrm{e}^{\pm j\, 0.69}$ and $p_{3,4} = 0.98\, \mathrm{e}^{\pm j\, 0.88}$. It describes a narrowband AR systems with close and sharp spectral peaks, at the frequencies $f_1 = 0.69/(2\pi) = 0.11$ and $f_2 = 0.88/(2\pi) = 0.14$ (see Fig. 3).

This model is particularly difficult to identify under low SNR conditions and poor estimates of the system parameters are obtained if the SNR is lower than 10 dB.

As a support of this assertion, a first Monte Carlo simulation of 100 independent runs have been carried out, by considering noisy sequences of $N = 1000$ samples. The variance of the observation noise has been fixed to $\sigma_w^* = 90$, corresponding to a SNR of about 10 dB.

The first four lines of Table 3 report the empirical means of the system parameter estimates together with the corresponding standard deviations, obtained with the considered methods. For the sake of simplicity, the estimates of σ_e^* and σ_w^* are

Table 2: True and estimated values of parameters and variances for Alg1-FD, Alg2-FD and Alg1-TD, Alg2-TD. SNR ≈ 10 dB and N=500.

	α_1	α_2	α_3	α_4	σ_e^*	σ_w^*	Time (ms)
True values	−2.1690	2.8227	−2.0408	0.8853	1	3.6	
Alg1 – FD (q = 8)	−2.1709 ± 0.0390	2.8332 ± 0.0488	−2.0462 ± 0.0264	0.8962 ± 0.0189	1.0482 ± 0.1415	3.6325 ± 0.0635	30.0
Alg1 – TD (q = 4)	−2.1757 ± 0.0432	2.8437 ± 0.0578	−2.0553 ± 0.0366	0.8997 ± 0.0203	0.9926 ± 0.0866	3.5734 ± 0.3117	7.5
Alg2 – FD (q = 4)	−2.1783 ± 0.0295	2.8488 ± 0.0628	−2.0615 ± 0.0574	0.9027 ± 0.0240	0.9300 ± 0.5373	3.5580 ± 0.3050	3.6
Alg2 – TD (q = 4)	−2.1793 ± 0.0247	2.8522 ± 0.0544	−2.0634 ± 0.0498	0.9025 ± 0.0220	0.9320 ± 0.5201	3.5980 ± 0.3069	1.0

not reported. It can be observed that Alg1-TD, Alg1-FD and Alg2-FD have unsatisfactory performances, with bad estimates of the parameters, while Alg2-TD exhibits a greater robustness against noise and still yields a satisfactory result.

In the previous simulations all the available N data, in the whole frequency range [0 0.5], have been used for the identification.

In the previous simulations all the available N data, in the whole frequency range [0 0.5], have been used for the identification.

However, it can be observed that the frequency domain methods Alg1-FD and Alg2-FD yield good parameter estimates when the system transfer function $G(e^{-j\omega_k})$, defined in (6), is identified by using only the data belonging to specific frequency windows defined by the user, $F_1 = [f_i,\ f_f]$ and $F_2 = [1 - f_f,\ 1 - f_i]$, with $f_i = \omega_i/(2\pi) \geq 0$ and $f_f = \omega_f/(2\pi) \leq 0.5$.

Remark 8. In the AR case, the input $e(t)$ is a white noise, equally persistently exciting at all frequencies. Thus, the choice of F_1 (and F_2) is linked only to the spectral properties of the AR system to be identified.

In particular, for the considered example, the window F_1 will contain the two frequencies f_1 and f_2 that characterize the four poles of model (88).

In order to verify this property, a second Monte Carlo simulation of 100 independent runs have been carried out, by considering again $N = 1000$ samples. However, the system transfer function $G(e^{-j\omega_k})$ has been identified by using only the $2L = 300$ frequencies in the windows $F_1 = [f_i,\ f_f]$ and $F_2 = [1 - f_f,\ 1 - f_i]$, where $f_i = 0.05$ and $f_f = 0.2$.

The last two lines of Table 3 report the identification results obtained with Alg1-FD and Alg2-FD. It can be observed that in this case both methods give good estimates of the AR parameters. It is quite surprising to observe that the computational efficiency of the algorithms is now improved, since only $2L < N$ data are used for the identification.

Remark 9. In the time domain, an equivalent filtering action requires the following operations: the determination, by inverse transform, of the time signal corresponding to the rectangular frequency windows F_1 and F_2 and the convolution of such signal with the time data sequence $y(t)$. The resulting filtered signal is then used in the identification algorithm. Not only are these operations less intuitive from a physical point of view, but they also increase in a significant way the computational burden of the identification procedure. This aspect is of particular importance in case these operations should be repeated several

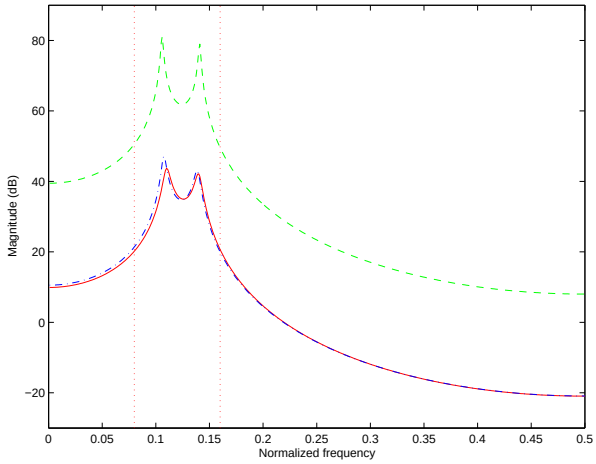

Figure 3: True TF: red, solid; Alg1-FD estimate: green, dashed; Alg2-FD estimate: blue, dash–dotted.

times, for example when the identification problem requires a trial–and–error procedure in order to obtain the best result, by changing the position and the width of the window F_1 in the frequency range [0 0.5]. Moreover, from simulation experiences, time domain filtering yields worse results for low SNR conditions.

Remark 10. The choice of the width of the window F_1 is linked to the value of σ_w^*. More amount of noise $w(t)$ is present on the data and more *a priori* information about the spectral properties of the AR system is required.

In particular, for the considered example, when σ_w^* increases a more accurate information about the exact positions of f_1 and f_2 is required.

As a proof of this assertion, other two Monte Carlo simulations of 100 independent runs have been carried out, with $N = 1000$. In this case, however, the variance of the observation noise has been fixed to $\sigma_w^* = 2700$, corresponding to a SNR of about -5 dB. Of course, under these very low SNR conditions also Alg2-TD completely fails the estimates; the results are not reported.

In the first simulation the system transfer function $G(e^{-j\omega_k})$ has been identified by using the same window $F_1 = [0.05\ 0.2]$, defined before. In the second simulation a more narrow window $F_1 = [0.08,\ 0.16]$ has been used, with a total number of $2L = 160$ frequencies.

The results of these simulations are reported in Table 4. It

Table 3: True and estimated values of the AR parameters for Alg1-FD, Alg2-FD and Alg1-TD, Alg2-TD. SNR ≈ 10 dB and N=1000.

	α_1	α_2	α_3	α_4	Time (ms)
True values	−2.7607	3.8106	−2.6535	0.9238	
Alg1 − FD ($q = 8$) $F_1 = [\,0 \quad 0.5\,]$	−2.0911 ± 0.5938	2.4295 ± 1.3386	−1.3965 ± 1.3103	0.5162 ± 0.5371	35.0
Alg1 − TD ($q = 4$)	−2.3307 ± 1.5771	2.7119 ± 3.9835	−1.5336 ± 4.0573	0.4498 ± 1.7307	28.2
Alg2 − FD ($q = 4$) $F_1 = [\,0 \quad 0.5\,]$	−2.1589 ± 1.2050	2.8041 ± 2.3264	−1.8611 ± 2.1528	0.7729 ± 0.8505	5.6
Alg2 − TD ($q = 4$)	−2.7820 ± 0.5854	3.9006 ± 1.0575	−2.7603 ± 0.9029	0.9813 ± 0.2983	1.2
Alg1 − FD ($q = 8$) $F_1 = [\,0.05 \quad 0.2\,]$	−2.7223 ± 0.0188	3.7624 ± 0.0315	−2.6323 ± 0.0247	0.9372 ± 0.0053	29.0
Alg2 − FD ($q = 4$) $F_1 = [\,0.05 \quad 0.2\,]$	−2.7434 ± 0.0802	3.7865 ± 0.2156	−2.6415 ± 0.2341	0.9305 ± 0.1232	2.6

Table 4: True and estimated values of the AR parameters and variance σ_e for Alg1-FD and Alg2-FD. SNR ≈ -5 dB and N=1000.

	α_1	α_2	α_3	α_4	σ_e^*	Time (ms)
True values	−2.7607	3.8106	−2.6535	0.9238	1	
Alg1 − FD ($q = 8$) $F_1 = [\,0.05 \quad 0.2\,]$	−2.5223 ± 0.0360	3.3818 ± 0.0469	−2.3656 ± 0.0303	0.8805 ± 0.0110	−−	35.0
Alg2 − FD ($q = 4$) $F_1 = [\,0.05 \quad 0.2\,]$	−2.5137 ± 0.2086	3.3189 ± 0.4673	−2.2576 ± 0.4652	0.8126 ± 0.2287	−−	2.6
Alg1 − FD ($q = 8$) $F_1 = [\,0.08 \quad 0.16\,]$	−2.8217 ± 0.0178	3.9402 ± 0.0254	−2.7838 ± 0.0171	0.9734 ± 0.0039	−−	32.5
Alg2 − FD ($q = 4$) $F_1 = [\,0.08 \quad 0.16\,]$	−2.8046 ± 0.0875	3.8866 ± 0.2017	−2.7181 ± 0.1996	0.9400 ± 0.0851	1.0465 ± 0.6050	2.0

can be observed that in the first simulation both methods yield worse estimates for the AR parameters, while in the second simulation they give good estimates, again. As a concluding remark, note that Alg2-FD has to be preferred to Alg1-FD. Not only it is faster, but it gives also a correct estimate of σ_e^*, while Alg1-FD completely fails this estimate, with a consequent error for the static gain of $|G(e^{-j\omega_k})|$, see Fig. 3. The estimates of σ_w^* are not reported, since completely wrong.

With reference to the last simulation, Figure 3 reports the true value of $|G(e^{-j\omega_k})|_{dB}$, together with the means of the transfer function estimates, obtained with Alg1-FD and Alg2-FD. The advantageous effects of filtering are evident for both methods, in fact they succeed in the identification of the two peaks of $|G(e^{-j\omega_k})|$ at the frequencies f_1 and f_2.

8. Conclusions

In this paper a novel frequency domain approach has been proposed for the identification of AR models affected by additive white noises. In particular, two different frequency domain algorithms have been proposed and their estimation properties have been tested and compared by means of Monte Carlo simulations. The numerical results have confirmed the good performances of the new methodology and have shown its effectiveness in the identification of narrowband AR systems with close and sharp spectral peaks.

Appendix A. Proof of Theorem 3

The maximal value of σ_s compatible with conditions (36) is obtained when $\sigma_w = 0$ and thus $\sigma_s = \sigma_e$. Starting from (38), the matrix $\Sigma_Y - \tilde{\Sigma}$ can be partitioned as

$$\Sigma_Y - \tilde{\Sigma} = \begin{bmatrix} \sigma_{11} - \sigma_s & \Sigma_{12} \\ \Sigma_{21} & \Sigma_{22} \end{bmatrix} \tag{A.1}$$

so that

$$\det(\Sigma_Y - \tilde{\Sigma}) = \det(\Sigma_{22}) \det(\sigma_{11} - \sigma_s - \Sigma_{12}\,\Sigma_{22}^{-1}\,\Sigma_{21}) . \tag{A.2}$$

Thus, from condition $\det(\Sigma_Y - \tilde{\Sigma}) = 0$, we obtain the maximal searched value

$$\sigma_s^{max} = \sigma_{11} - \Sigma_{12}\,\Sigma_{22}^{-1}\,\Sigma_{21} = \frac{\det(\Sigma_Y)}{\det(\Sigma_{22})} . \tag{A.3}$$

The maximal value of σ_w compatible with conditions (36) is obtained by assuming $\sigma_e = 0$ in (35), so that it results

$$\tilde{\Sigma} = \mathrm{diag}\,[\,\sigma_w\, I_{n+1},\, 0_n\,] . \tag{A.4}$$

Starting from (40), the matrix $\Sigma_Y - \tilde{\Sigma}$ can be partitioned as

$$\Sigma_Y - \tilde{\Sigma} = \begin{bmatrix} \Sigma_{11} - \sigma_w\, I_{n+1} & \Sigma_{12} \\ \Sigma_{21} & \Sigma_{22} \end{bmatrix} \tag{A.5}$$

so that

$$\begin{aligned} &\det(\Sigma_Y - \tilde{\Sigma}) = \\ &\det(\Sigma_{22}) \det(\Sigma_{11} - \sigma_w\, I_{n+1} - \Sigma_{12}\,\Sigma_{22}^{-1}\,\Sigma_{21}) . \end{aligned} \tag{A.6}$$

Conditions (36) are thus satisfied if and only if

$$\Sigma_{11} - \sigma_w\, I_{n+1} - \Sigma_{12}\,\Sigma_{22}^{-1}\,\Sigma_{21} \geq 0 \tag{A.7}$$

which leads immediately to (41). ◊

Appendix B. Proof of Theorem 4

Let $\tilde{\Sigma}(P) = \mathrm{diag}\,[\,\sigma_s,\, \sigma_w\, I_n,\, 0_n\,]$. Since both ξ and P belong to r it follows that $\xi = \lambda\, P$. Moreover, the coordinates (σ_s, σ_w) of P must satisfy the conditions

$$\Sigma_Y - \tilde{\Sigma}(P) \geq 0 \qquad \det\left(\Sigma_Y - \tilde{\Sigma}(P)\right) = 0 \tag{B.1}$$

so that

$$\det \Sigma_Y^{-1} \left(I_{2n+1} - \frac{1}{\lambda} \Sigma_Y^{-1} \tilde{\Sigma}_\xi \right) = 0 \,, \tag{B.2}$$

where $\tilde{\Sigma}_\xi$ is defined in (44). Thus, the scalar λ that solves (B.2) is given by

$$\lambda_M = \max \text{ eig} \left(\Sigma_Y^{-1} \tilde{\Sigma}_\xi \right) \,. \tag{B.3}$$

Consequently, the coordinates of point P are given by (42). $\Diamond$

References

[1] L. Marple, *Digital Spectral Analysis with Applications*, Prentice–Hall, Englewood Cliffs, New Jersey, 1987.

[2] S. M. Kay, *Modern Spectral Estimation*, Prentice–Hall, Englewood Cliffs, New Jersey, 1988.

[3] P. Stoica and R. Moses, *Introduction to Spectral Analysis*, Prentice–Hall, Upper Saddle River, New Jersey, 1997.

[4] R. Pintelon and J. Schoukens, Time series analysis in the frequency domain, *IEEE Transactions on Signal Processing*, 47 (1999) 206–210.

[5] P. Van Overschee, B. De Moor, W. Dehandschutter and J. Swevers, A subspace algorithm for the identification of discrete time frequency domain power spectra. *Automatica*, 33 (1997) 2147–2157.

[6] L. Ljung, *System identification–Theory for the user* (2nd ed.), Prentice–Hall, Upper Saddle River, New Jersey, 1999.

[7] R. Pintelon and J. Schoukens, *System identification: a frequency domain approach* (2nd ed.), IEEE Press, New York, 2012.

[8] S. M. Kay, The effects of noise on the autoregressive spectral estimator. *IEEE Transactions on Acoustics, Speech and Signal Processing*, 27 (1979) 478–485.

[9] M. Pagano, Estimation of models of autoregressive signal plus white noise. *The Annals of Statistics*, 2,(1974) 99–108.

[10] A. Nehorai and P. Stoica, Adaptive algorithms for constrained ARMA signals in the presence of noise. *IEEE Transactions on Acoustics, Speech and Signal Processing*, 36 (1988) 1282–1291.

[11] Y.T. Chan and R.P. Langford, Spectral estimation via the high–order Yule–Walker equations. *IEEE Transactions on Acoustics, Speech and Signal Processing*, 30 (1982) 689–698.

[12] J. Cadzow, J. Spectral estimation: an overdetermined rational model equation approach. *Proceedings of the IEEE*, 70 (1982) 907–939.

[13] S. M. Kay, Noise compensation for autoregressive spectral estimates. *IEEE Transactions on Acoustics, Speech and Signal Processing*, 28 (1980) 292–303.

[14] T. Sen Lee, Large sample identification and spectral estimation of noisy multivariate autoregressive processes. *IEEE Transactions on Acoustics, Speech and Signal Processing*, 31 (1983) 76–82.

[15] K.K. Paliwal, A noise–compensated long correlation matching method for AR spectral estimation of noisy signals. *Signal Processing*, 15 (1988) 437–440.

[16] C. E. Davila, A subspace approach to estimation of autoregressive parameters from noisy measurements. *IEEE Transactions on Signal Processing*, 46 (1998) 531–534.

[17] H. Sakai and M. Arase, Recursive parameter estimation of an autoregressive process disturbed by white noise. *International Journal of Control*, 30 (1979) 949–966.

[18] W.X. Zheng, Fast identification of autoregressive signals from noisy observations. *IEEE Transactions on Circuits and Systems–II*, 52 (2005) 43–48.

[19] A. Mahmoudi and M. Karimi, Inverse filtering based method for estimation of noisy autoregressive signals. *Signal Processing*, 91 (2011) 1659–1664.

[20] L.-J. Jia, S. Kanae, Z.-J. Yang and K. Wada, On bias compensation estimation for noisy AR process. *Proc. of the 42–nd IEEE Conference on Decision and Control*, Maui, Hawaii, USA, 2003, 405–410.

[21] R. Diversi, R. Guidorzi and U. Soverini, A new estimation approach for AR models in presence of noise. *Preprints of the 16-th IFAC World Congress* Prague, Czech Republic, 2005.

[22] R. Diversi, R. Guidorzi and U. Soverini, A noise–compensated estimation scheme for AR processes. *Proc. of the 44-th IEEE Conference on Decision and Control and 8–th European Control Conference* Seville, Spain, 2005, 4146–4151.

[23] R. Diversi, R. Guidorzi and U. Soverini, Identification of autoregressive models in the presence of additive noise. *Int. Journal of Adaptive Control and Signal Processing*, 22 (2008) 465–481.

[24] S. Beghelli, R. Guidorzi and U. Soverini, The Frisch scheme in dynamic system identification. *Automatica*, 26 (1990) 171–176.

[25] R. Guidorzi, R. Diversi and U. Soverini, The Frisch Scheme in algebraic and dynamic identification problems. *Kybernetika*, 44 (2008) 585–616.

[26] R. Pintelon, J. Schoukens and G. Vandersteen, Frequency domain system identification using arbitrary signals. *IEEE Transactions on Automatic Control*, 42 (1997) 1717–1720.

[27] J.C. Agüero, J.I. Yuz, G.C. Goodwin and R.A. Delgado, On the equivalence of time and frequency domain maximum likelihood estimation. *Automatica*, 46 (2010) 260–270.

[28] T. McKelvey, Frequency domain identification methods. *Circuits Systems Signal Processing*, 21 (2002) 39–55.

[29] U. Soverini and G. Catania, FRF parameter identification with arbitrary input sequence from noisy input-output measurements. *Proc. of the 21–st MTNS*, Groningen, The Netherlands, 2014, 551–556.

[30] U. Soverini and T. Söderström, Frequency domain maximum likelihood identification of noisy input–output models. *Proc. of the 19–th IFAC World Conference*, Cape Town, South Africa, 2014, 4625–4630.

[31] U. Soverini and T. Söderström, Frequency domain EIV identification: a Frisch Scheme approach. *Proc. of the 19–th IFAC World Conference*, Cape Town, South Africa, 2014, 4631–4636.

[32] C.E. Davila, On the noise–compensated Yule–Walker equations. *IEEE Transactions on Signal Processing*, 49 (2001) 1119–1121.

[33] S. Van Huffel and J. Vandewalle, Comparison of total least squares and instrumental variable methods for parameter estimation of transfer function models. *International Journal of Control*, 50 (1989) 1039–1056.

[34] T. Söderström, Errors–in–Variables methods in system identification. *Automatica*, 43 (2007) 939–958.

[35] F. Tisseur and K. Meerbergen, The quadratic eigenvalue problem. *SIAM Review*, 43 (2001) 235–286.